INTERNATIONAL JOURNAL OF CLIMATOLOGY
Int. J. Climatol. **30**: 236–255 (2010)
Published online 25 February 2009 in Wiley InterScience
(www.interscience.wiley.com) DOI: 10.1002/joc.1882

RMetS
Royal Meteorological Society

A hydroclimatic index for examining patterns of drought in the Colorado River Basin

Andrew W. Ellis,[a]* Gregory B. Goodrich[b] and Gregg M. Garfin[c]
[a] *School of Geographical Sciences, Arizona State University, Tempe, Arizona, USA*
[b] *Department of Geography and Geology, Western Kentucky University, Bowling Green, Kentucky, USA*
[c] *Institute for the Study of Planet Earth, University of Arizona, Tucson, Arizona, USA*

ABSTRACT: To better understand drought occurrence in the Colorado River Basin (CRB) of the southwestern United States we used a hydroclimatic index to create a historical record of drought coverage and analysed the linear trend and relationships with key climate teleconnections. The past century was characterized by an increase in drought coverage during the warm portion of the year almost exclusively as a result of climatic warming. In recent decades, a significant increase in the drought coverage occurred earlier in the year, during the spring season, primarily as a function of warming, but in combination with a decline in precipitation for a significant portion of the basin. The El Niño (La Niña) phase of the El Niño-Southern Oscillation (ENSO) phenomenon is associated with a smaller (larger) area of drought during fall and winter, and the ENSO phase during the preceding six months is a significant predictor. The area of drought within the CRB is larger (smaller) during the warm (cold) phases of the Atlantic Multi-decadal Oscillation (AMO) and the Pacific Decadal Oscillation (PDO), although the relationship with the PDO is weak. Monthly AMO values for the two years preceding drought provide minor predictability. Decadal averages of drought coverage closely follow those of both the AMO and PDO index. However, the nature of the PDO-drought relationship is reversed over the two halves of the historical record, possibly indicating a dominance of the AMO over the PDO in influencing drought in the region. Teleconnection-drought relationships are stronger for the southern portion of the basin. Trends in drought coverage, the current phases of the AMO and PDO, climate change projections of regional warming, and the likelihood of continued rapid population growth could result in significant water resource problems within the CRB. Copyright © 2009 Royal Meteorological Society

KEY WORDS drought; Colorado River Basin; trends; teleconnection

Received 28 July 2008; Revised 24 January 2009; Accepted 24 January 2009

1. Introduction

1.1. Drought and the Colorado River Basin

Drought causes greater economic impact than any other natural hazard, with an estimated $6–8 billion in annual losses in the United States alone (Wilhite *et al*., 2005). Since 2000, southwestern states have exhibited a variety of drought impacts, including over 2.6 million acres of Arizona and New Mexico conifer damaged from a combination of severe drought stress and enhanced insect pest outbreaks (USDA Forest Service, 2004; Breshears *et al*., 2005), substantial increases in acres burned in the Colorado River Basin (CRB) states, water restrictions in major metropolitan areas such as Las Vegas and Denver (e.g. Kenney *et al*., 2004), water shortages in vulnerable rural regions and on tribal lands, and substantial livestock losses. The rapidly growing population of the southwestern United States is particularly sensitive to drought because of the reliance on water from the relatively arid CRB and over-allocated Colorado River. Since 2000, prolonged declines in Colorado River reservoir storage have sensitized regional water managers to the increasingly likely possibility of drought-related shortages (McCabe and Wolock, 2007; Garrick *et al*., 2008). Regional cities and states had been engaged in unprecedented drought planning, and the seven CRB states developed the first-ever shortage criteria for reservoir operations (USDOI, 2007).

The CRB encompasses an area of approximately 634 550 km^2 that stretches across the southwestern United States (626 780 km^2 of the CRB) and northwestern Mexico (7770 km^2), and is drained by the Colorado River and its tributaries. Originating in the high elevations of Colorado and flowing southwestward for 2366 km to the Gulf of California, the Colorado River drains parts of seven states (Figure 1). The 1922 Colorado River Compact divided the river into an upper basin (UB) and lower basin (LB) that approximate two halves of the CRB, with the LB slightly larger at around 55% of the area. Positioned at a lower mean latitude and elevation, the LB is much warmer than the UB annually, with the greatest difference during the cool season (Figure 2(a)). Nearly 60% of the area of the UB is at an elevation greater than 2 km compared to only about 16% of the LB. Annual precipitation for the two

* Correspondence to: Andrew W. Ellis, School of Geographical Sciences, Arizona State University, USA. E-mail: dellis@asu.edu

Figure 1. The Colorado River Basin (adapted from the Colorado River Commission of Nevada (http://crc.nv.gov)). This figure is available in colour online at www.interscience.wiley.com/ijoc

sub-basins is not dramatically different (within 20%); however, monthly differences are large during spring and early summer (April–June) when the UB is considerably wetter than the LB (Figure 2(b)). During mid- to late-summer (July–August) the pattern is reversed and the LB is wetter than the UB (Figure 2(b)), as the North American monsoon circulation transports moisture northward into the region initiating convective precipitation.

The Colorado River is a critical source of water for the southwestern United States; as a result the river is highly dammed. More water is exported from the CRB than from any other basin in the United States in meeting the municipal and industrial demands of more than 24 million people that are predominantly located in urban areas across the Southwest. Still, the high-population density urban areas represent a small fraction of the CRB, and in fact 75% of the CRB is comprised of protected land. Dammed rivers and large surface water reservoirs are important in the CRB due to the aridity of the region, the high-interannual variation in precipitation and runoff, and the propensity for multi-year drought. The mean potential evapotranspiration (PE), or climatic demand for water, is high for both basins (Figure 2(c)), and approximately one and a half times greater annually in the LB compared to the UB due to the lower latitude (greater annual solar radiation) and higher air temperature (Figure 2(a)) of the LB. The contrast between climatic demand for water and natural water availability, or precipitation (P), puts drought stress in perspective. On a mean monthly basis, values of P-PE are positive only for the months of November through March in the UB and December through January in the LB (Figure 2(d)). Although this amount of 'available water' varies inter-annually and spatially across the basins, the mean values demonstrate the need to capture and store runoff for municipal needs.

The regional climate of the CRB has changed over the past century. On average, mean annual air temperature increased by nearly 1.3 °C across the 112-year period 1895–2006, and the rate of warming was even greater over the last 30 years (Figure 3(a)). The record of precipitation across the CRB is not characterized by a long-term linear trend (Figures 3(b) and (c)), but there are periods of a significant trend, including a decline in the LB over the past 30 years (Figure 3(b)). The potential impacts of future climate change on runoff within the CRB have

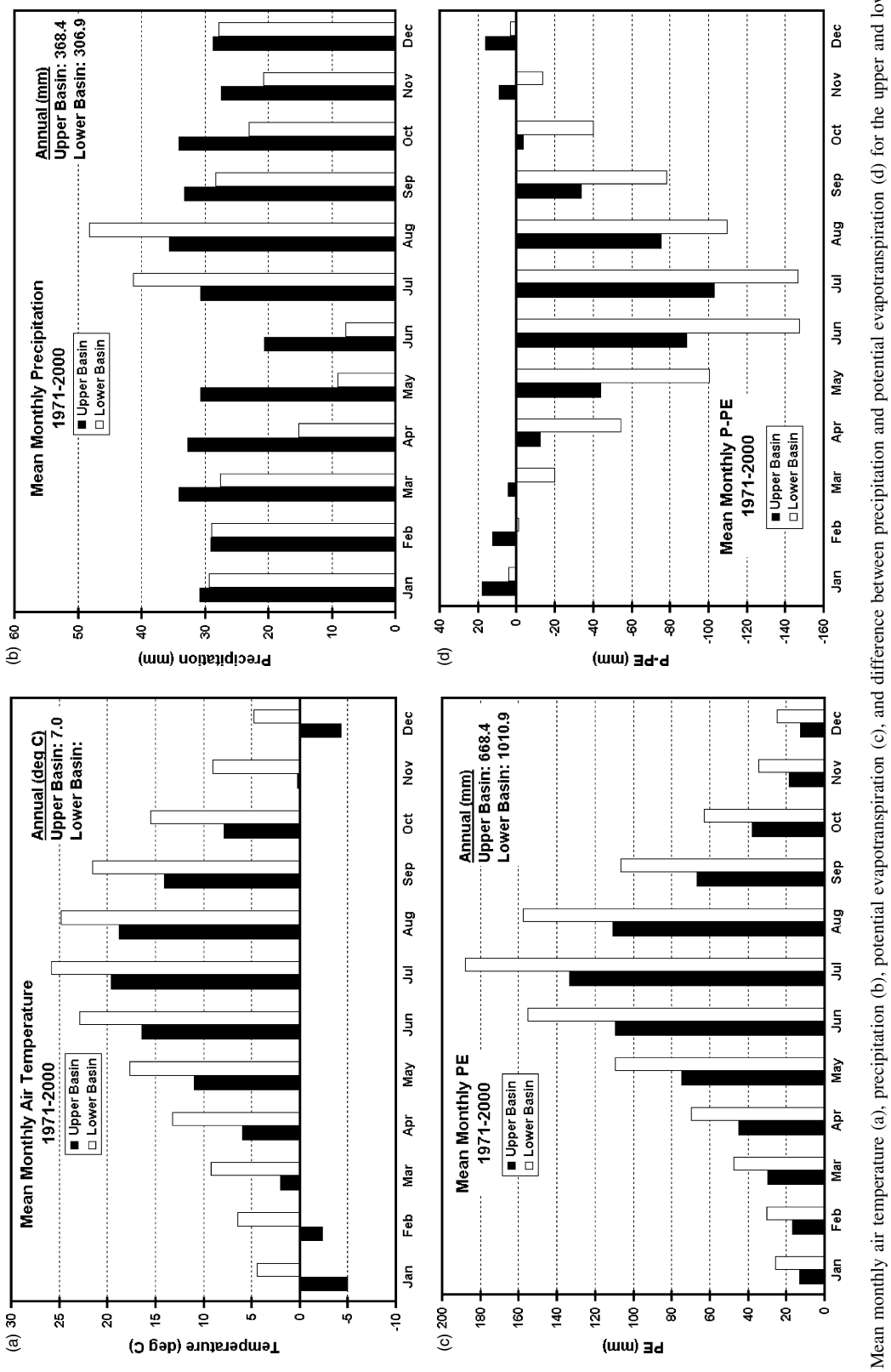

Figure 2. Mean monthly air temperature (a), precipitation (b), potential evapotranspiration (c), and difference between precipitation and potential evapotranspiration (d) for the upper and lower basins.

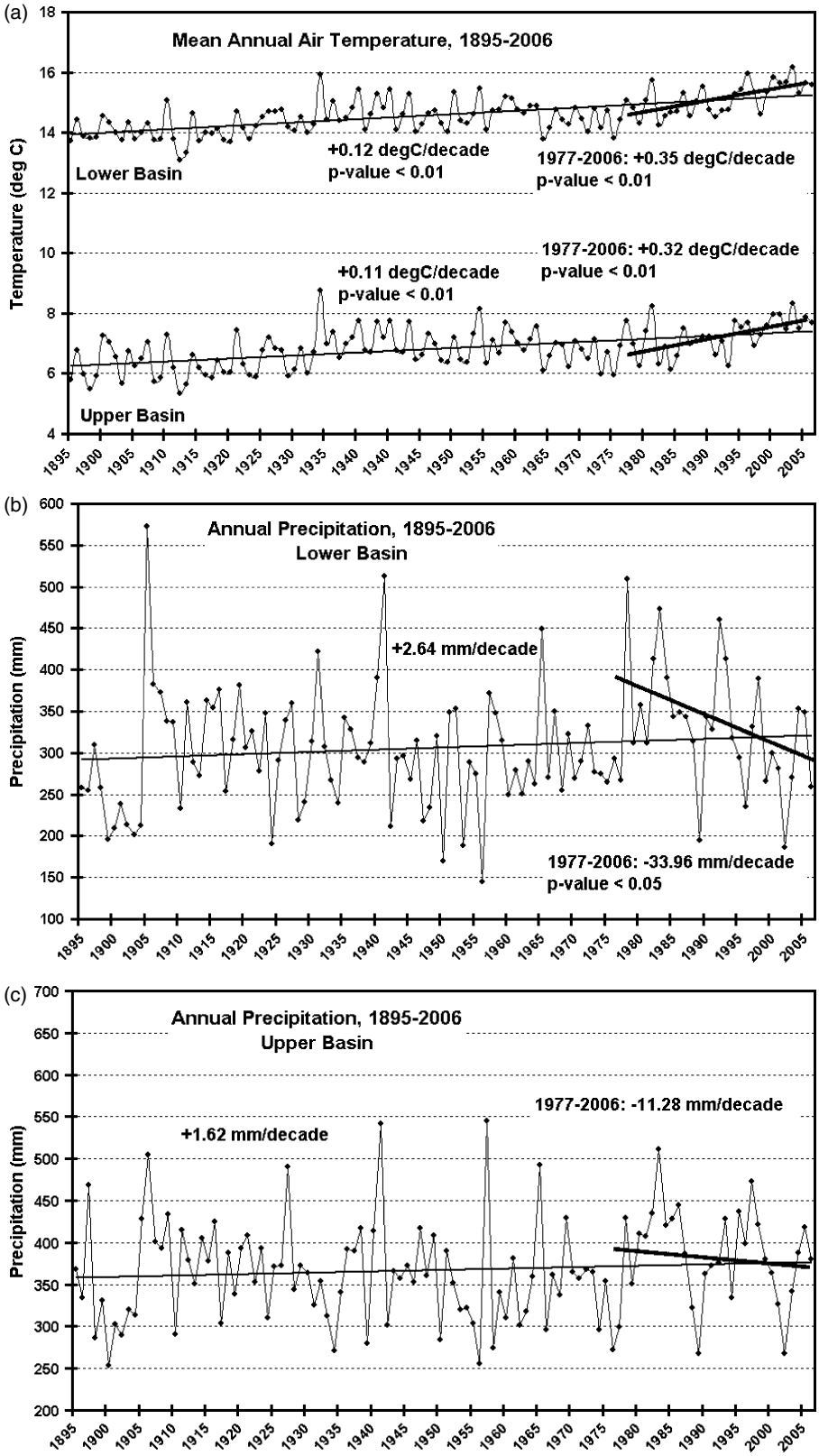

Figure 3. Time series of mean annual air temperature for the lower and upper basins (a) and precipitation for the lower (b) and upper (c) basins.

been outlined in at least nine major studies over the past 25 years (Revelle and Waggoner, 1983; Nash and Gleick, 1991, 1993; Christensen *et al*., 2004; Milly *et al*., 2005; Christensen and Lettenmaier, 2006; Hoerling and Eischeid, 2006; Seager *et al*., 2007; Ellis *et al*., 2008). Each of these studies signalled a likelihood of significant reductions in runoff within the basin in response to warmer and drier conditions, particularly during winter months. The projections are compounded by the certainty that the population of the region will continue to increase.

To better understand drought occurrence in the CRB we established the record of the spatial coverage of drought over the past century, or approximately the instrumental period of record. Specifically we focus on linear trends for the two sub-basins of the CRB and on the relationship between temporal patterns and major climate teleconnections that have been linked to the climate of the region. This required that we define drought and represent its occurrence across the CRB.

1.2. Defining drought occurrence

It is well documented that indexing drought is difficult and that most drought indices used in monitoring are characterized by regional biases and limited relationships to the multiple dimensions of drought (e.g. Heim, 2002; Keyantash and Dracup, 2002; Steinemann *et al*., 2005). The Palmer Drought Severity Index (PDSI) (Palmer, 1965) is arguably the most widely used drought indicator during the past 50 years. The PDSI is derived from a moisture balance model and reflects how soil moisture compares with the average condition. A given PDSI value is a combination of the current condition and the previous PDSI value, reflecting the trend in soil moisture. Many authors (e.g. Dickerson and Dethier, 1970; Alley, 1984; Karl, 1986; Heddinghaus and Sabol, 1991; Guttman *et al*., 1992; Lohani *et al*., 1998; Steinemann, 2003) have identified significant weaknesses in the PDSI. Foremost is the fact that the empirical relationships specified in Palmer's water balance model for determining drought severity, onset and end were developed from field experiments specific to the Midwestern region of the United States (Palmer, 1965). Application of the PDSI to regions with climatic characteristics that are very different from those of the Midwest is potentially problematic. Another major problem is that the PDSI is based on departures from average, without consideration of precipitation variability, and therefore it tends to perform poorly in regions with high inter-annual variability (Steinemann *et al*., 2005).

Alternative versions of the PDSI that employ the basic water budget equation, such as the Palmer Hydrological Drought Index (PHDI), Weighted PDSI and the Self-Calibrated PDSI (Wells *et al*., 2004) exhibit regional biases similar to those in the basic PDSI. Other indices address specific sectors impacted by drought, such as the Crop Moisture Index (Palmer, 1968) for agriculture and the Surface Water Supply Index (Shafer and Dezman, 1982; Doesken and Garen, 1991) for water resources. Since each of these drought indices uses different variables to represent supply and demand within the water budget equation to satisfy its own sector-specific definition, there are often different results between indices during the same drought period for a given location.

The Standardized Precipitation Index (SPI) (McKee *et al*., 1993, 1995) is preferred to the PDSI by many climatologists. The SPI quantifies precipitation anomalies for multiple time scales. SPI calculations commonly fit the long-term record to a gamma distribution and then transform the data to a normal distribution, in order to facilitate comparisons across regions, using a scale with a common interpretation. Thus, a value of zero corresponds to the median, and departures relate directly to the well-known normal distribution. Despite satisfying many of the concerns associated with the PDSI, the SPI only considers one-half of the hydrologic equation, ignoring the temperature-driven climatic demand for water (PE). This is a critical problem in climates with an extremely warm summer season, during which evaporative loss can dominate the hydrologic budget (e.g. Figure 2(d)) despite significant precipitation (e.g. Figure 2(b)). It is also problematic in climates characterized by months that are reliably arid, such that a single-precipitation event can dominate monthly SPI calculations. In such climates, summer precipitation is much less 'effective' than cooler winter season precipitation for replenishing soil moisture and water supplies. Furthermore, by not representing the loss of water to the atmosphere, the SPI cannot account for the impacts of climate change in the form of atmospheric warming.

What we call the 'hydroclimatic index' (HI) is a representation of the difference between measured precipitation (P) and estimated PE, in the form P-PE. This concept dates back to the 'aridity index' of Thornthwaite's climate classification work in the late 1940s (Thornthwaite, 1948), which was based on P-PE from only months with negative values. More recently the United Nations Environment Programme calculated an aridity index as a ratio of the two variables (P/PE) in mapping desertification (UNEP, 1992). In recent decades the P *versus* PE concept has been applied predominantly in agriculture.

The HI avoids difficulties associated with using actual evapotranspiration (AE), which varies with soil moisture content and the capacity of the soil to retain water (i.e. field capacity). Using P-PE also allows for comparison of the hydroclimatic conditions across different regions, since PE is not limited by soil moisture. PE represents water loss from a soil that is continuously at field capacity, which also de-emphasizes the importance of soil type. The HI represents the hydroclimatic condition at any point in time from which varying degrees of drought can be identified.

1.3. Major climate teleconnections to the Southwest

It is well known that year-to-year variability in precipitation across the United States is forced primarily from sea surface temperature (SST) anomalies in the tropical Pacific Ocean, known as the El Niño-Southern Oscillation (ENSO phenomenon (Ropelewski and Halpert, 1986), and that drought in the Southwest is linked to the cold phase of ENSO, or La Niña (Redmond and Koch, 1991; Piechota and Dracup, 1996; Cayan *et al*., 1999).

The Pacific Decadal Oscillation (PDO) is an ENSO-like pattern of northern Pacific Ocean SST variability with a periodicity of around 50 years (Mantua and Hare, 2002). Positive (warm phase) values of the PDO refer

to above normal SSTs along the west coast of North America and along the equator, and below normal SSTs in the central and western North Pacific centred around 45° of north latitude. Negative (cold phase) values of the PDO refer to the opposite distribution of SSTs in these same areas. The dynamic mechanism that forces variability of the PDO remains uncertain. It is well known that the usefulness of ENSO as a seasonal predictive tool varies with the phase of the atmosphere-ocean variations in the Pacific, as measured by the PDO index (Gershunov and Barnett, 1998; McCabe and Dettinger, 1999; Gutzler *et al*., 2002; Brown and Comrie, 2004).

The Atlantic Multi-decadal Oscillation (AMO) is a mode of natural variability occurring primarily in SSTs in the northern Atlantic Ocean with a periodicity of 60–80 years. The warm phase of the AMO has been associated with negative precipitation anomalies in the central and western United States, such as the droughts of the 1930s and 1950s (Enfield *et al*., 2001; Hidalgo, 2004; McCabe *et al*., 2004). Since 1998, the AMO has returned to the warm phase and drought has returned to much of the western/southwestern United States.

2. Methods

2.1. Hydroclimatic index

We extracted historic (1895–2006) mean monthly maximum and minimum air temperature values and total monthly precipitation values across the CRB from the Parameter-elevation Regressions on Independent Slopes Model (PRISM) dataset (Daly *et al*., 1994) (http://www.prism.oregonstate.edu). The resolution of the PRISM grid is 0.0416° of latitude and longitude (approximately 4 km), yielding 37 810 grid cells within the bounds of the CRB.

To test the applicability of PRISM data, we downloaded monthly mean air temperature and total precipitation data for stations in the United States Historical Climate Network (USHCN; Easterling *et al*., 1996). Data are available for 1221 stations from the United States National Climatic Data Center and the Carbon Dioxide Information Analysis Center of the Oak Ridge National Laboratory (http://cdiac.ornl.gov/epubs/ndp/ushcn/newushcn.html). There are 57 USHCN stations within the CRB, and we gathered data for the 52 stations with a 90 year or greater period of record, as the number of stations with a record length of at least 100 years significantly decreases to 37. We further reduced the number of stations by retaining only those with no missing data, resulting in 42 and 43 stations with temperature and precipitation data respectively. From the PRISM data set we extracted monthly data for the grid cell closest to each USHCN station for comparison. The mean absolute difference between PRISM and USHCN data for each station was calculated (Table 1), and the values reveal rather good agreement for both temperature and precipitation. Furthermore, to generally determine if PRISM data are appropriate for use in time series analysis, we calculated the 90-year linear trend in the USHCN and PRISM data for each station and its corresponding grid cell and compared the two sets of trends using a paired t-test. The results (Table 2) suggest that the trends associated with the two data sets are not significantly different for either air temperature (p-value 0.49) or precipitation (p-value 0.62).

We used the raw PRISM precipitation data in the calculation of the HI (P-PE), and estimated monthly PE using mean monthly temperature data calculated from the PRISM maximum and minimum temperatures. On the basis of the results of previous tests of several methods of PE calculation within the CRB (Ellis *et al*., 2008), we

Table I. Mean values of the descriptive statistics of the monthly mean absolute difference between USHCN station data and the corresponding PRISM grid cell data for mean air temperature (T; $n = 42$) and precipitation (P; $n = 43$).

	Mean		SD		LQ		Median		UQ	
	T	*P*	*T*	*P*	*T*	*P*	*T*	*P*	*T*	*P*
Jan	1.2	5.0	1.3	6.6	0.5	0.8	0.8	2.5	1.2	6.0
Feb	1.2	5.2	1.4	7.7	0.5	0.9	0.8	2.1	1.3	6.0
Mar	1.2	5.4	1.5	8.0	0.5	1.0	0.7	2.1	1.2	6.6
Apr	1.2	4.3	1.6	7.0	0.5	0.7	0.7	1.6	1.2	4.3
May	1.3	3.0	1.7	4.2	0.6	0.6	0.8	1.6	1.2	4.1
Jun	1.3	2.0	1.8	1.7	0.6	0.7	0.8	1.4	1.1	2.8
Jul	1.3	5.8	1.6	5.5	0.5	1.6	0.8	4.0	1.2	8.3
Aug	1.3	6.1	1.6	5.5	0.6	2.0	0.8	4.3	1.2	9.1
Sep	1.3	4.6	1.5	4.6	0.6	1.6	0.8	2.9	1.2	6.1
Oct	1.2	4.0	1.4	4.6	0.6	1.1	0.8	2.4	1.1	4.9
Nov	1.1	4.0	1.2	5.7	0.6	0.6	0.7	2.0	1.0	3.7
Dec	1.1	4.8	1.2	6.6	0.5	0.9	0.7	2.4	1.1	5.8
Ann	1.2	4.5	1.5	5.6	0.5	1.1	0.7	2.5	1.2	5.7

Included are the mean, median, standard deviation (SD) and lower (LQ) and upper quartiles (UQ).

Table II. Paired t-test results comparing linear trends (1917–2006) from USHCN stations and corresponding PRISM grid cells for monthly mean air temperature (T; $n = 42$) and total precipitation (P; $n = 43$).

T	Mean	SD	SE Mean
USHCN	0.145	0.115	0.018
PRISM	0.158	0.084	0.013
Difference	−0.013	0.123	0.019
t-Value = −0.70		p-Value = 0.49	

P	Mean	SD	SE Mean
USHCN	0.052	0.468	0.071
PRISM	0.083	0.514	0.078
Difference	−0.031	0.408	0.062
t-Value = −0.51		p-Value = 0.62	

Included are the mean, standard deviation (SD), and standard error (SE) of the mean in units of degrees Celsius (T) or millimeters (P) per decade.

employed the Hamon (1961) method for PE estimation. The Hamon equation for PE (mm/month) is

$$PE = 13.97 d D^2 W_t \quad (1)$$

where d is the number of days in a month, D is the mean monthly hours of daylight in units of 12 h, and W_t is a saturated water vapour density term, which is calculated as

$$W_t = \frac{4.95 e^{0.062T}}{100} \quad (2)$$

where T is mean monthly temperature (°C) (Wolock and McCabe, 1999). The Hamon method has been tested and used in many research applications (e.g. Federer and Lash, 1983; Federer *et al*., 1996; Wolock and McCabe, 1999; Xu and Singh, 2001; Sun *et al*., 2002; Legates and McCabe, 2005; Lu *et al*., 2005).

Once we calculated the time series of monthly P-PE values for each grid cell in the CRB, we calculated aggregates of P-PE for an array of timeframes that were chosen to represent short-term (1-, 3-, 6-month), intermediate (12-, 24-month), and long- term drought conditions (36-, 48-month). However, since the serial correlation within the time series of the 24-, 36- and 48-month values is significant, we focus our analyses on the timeframes of 12 months and less. The P-PE values for each timeframe were converted to percentiles by month, relative to the 112-year period of record, to form the HI as a representation of the historical hydroclimatic conditions for each grid cell at any point in time.

2.2. Drought area

Using drought category thresholds established in creating the Arizona Drought Monitor (http://www.azwater.gov/dwr/drought/DroughtStatus.html) in consultation with scientists at the United States National Drought Mitigation Center (NDMC), we stratified HI values through the period of record for each grid cell within the CRB. Using the area of each cell, we calculated the percentages of the CRB and its UB and LB characterized by different levels of drought. We created time series of the area affected by: abnormal dryness (≤40th percentile), moderate drought or worse (≤25th percentile), severe drought or worse (≤15th percentile), and extreme drought (≤5th percentile). This approach is similar to that of Cook *et al*. (2004) who constructed a Drought Area Index using PDSI values on a 2.5° resolution across the western United States. Likewise, it is similar to the severity-area-duration methodology of Andreadis *et al*. (2005) in which they incorporated a hydrologic model to simulate soil moisture and runoff on a 0.5° resolution across the United States.

Mean values of the area within the CRB affected by the different categories of drought approximate the percentile thresholds that define the drought categories. For instance, the mean percentage of the CRB characterized by moderate drought or worse, or of the 25th percentile or lower, is approximately 25%. The drought area data are positively skewed, which is not surprising since they characterize just 40% or less of the hydroclimatic record in representing only historically dry conditions. The area of drought in the two basins has co-varied historically, as correlation coefficients for each degree of drought and for each of the time frames are positive, ranging from 0.62 to 0.75, and highly significant (p-values ≤0.01). However, in this study we examine the UB and LB separately in order to explore subtle differences in the time series of the area of drought.

2.3. Trends in drought area

We calculated linear trends in drought coverage for the different timeframes for the UB and LB. Raw data were used in linear regression analysis to construct the slope of the trend line (percent per year), but we tested each time series for normality using the Kolmogorov-Smirnov test and transformed non-normal distributions using the normal scores function in the Minitab statistical software package (version 13.20) prior to determining the significance of the trend. We conducted the trend analyses for the period of record (1895–2006) and for the most recent 30-year period (1977–2006), the latter of which was characterized by significant warming across the two basins (Figure 3(a)) and a significant decreasing trend in precipitation within the LB (Figure 3(b)). However, the trends in temperature and precipitation are obviously not monotonic, and therefore trends and their significance are dependent upon the time period chosen.

Next, we attempted to determine the amount of the trend in drought area that is explained by air temperature and precipitation by isolating the trend and eliminating the variability. We used the linear regression equations from the trend analysis to generate linear time series of drought area for each of the timeframes, and we compared these estimated data with time series of basin-averaged mean temperature and total precipitation to determine the degree to which each variable relates to trends in drought. We tested temperature and precipitation independently using regression analysis to determine the percentage of variance in the trend in drought coverage explained by each variable. We also calculated linear trends in basin-averaged temperature, precipitation, and PE.

2.4.. Relationships with climate teleconnections

We examined the area of drought for relationships with well-documented climate system teleconnections that exhibit statistically significant associations with climate variability in the western United States. To represent relatively short-term climate oscillations, we focused on the ENSO ocean-atmosphere phenomenon. We also examined multi-decade climate oscillations using the PDO and the AMO.

In this study, the phase and strength of the ENSO phenomenon is represented by the Multivariate El Niño-Southern Oscillation Index (MEI). The MEI is a comprehensive representation of ENSO in the

form of the first unrotated principal component of six observed variables combined (Wolter and Timlin, 1993). The data are available from the United States National Oceanic and Atmospheric Administration's Earth System Research Laboratory (http://www.cdc.noaa.gov/people/klaus.wolter/MEI/).

The PDO index is defined as the leading principal component of northern Pacific Ocean monthly SST variability poleward of 20°N latitude. The data are available from the Joint Institute for the Study of the Atmosphere and Ocean at the University of Washington (http://jisao.washington.edu/pdo/PDO.latest). AMO data are available from the NOAA Environmental Research Laboratory (http://www.cdc.noaa.gov/Timeseries/AMO/), and in this case they represent unsmoothed, de-trended SSTs generated from the Kaplan SST data base, version 2.

To examine short-term teleconnection-drought relationships, we stratified the area of drought data by ENSO phase using the MEI. The 684 monthly MEI values (1950–2006) were ordered and divided into thirds, with the upper third ($\geq+0.457$) representing El Niño conditions and the lower third (≤-0.351) representing La Niña conditions. Any season or year was categorized within a particular phase if at least half of the individual months were in that phase. To assess the significance of the difference in the area of drought during the two ENSO phases, we subjected the two data populations to a two-sample *t*-test. To assess the MEI as a predictive tool we calculated the variance in the area of drought explained by the index. We focused on the monthly MEI values for the 12 months leading up to each timeframe with a statistically significant difference in drought during the two ENSO phases. Regression analysis was used to determine the explained variance values, and for any data series with a significant time-dependent linear trend, we used the residuals from the trend line in the correlation analysis. We normalized all non-normal data prior to conducting the analysis.

Similar to the MEI-drought analysis, we stratified the area of drought data by phase of the PDO and AMO and subjected them to a two-sample *t*-test. For the PDO, we used a continuous series of warm phase (1925–1946 and 1977–2006) and cool phase (1895–1924 and 1947–1976) years, based on work by Mantua *et al*. (1997) and Zhang *et al*. (1997). Extending the recent warm phase through the end of the record is debatable since there is some evidence of a transition to a cool phase beginning in 1998. Without definitive evidence we continued the warm phase through 2006. For the AMO, we used the warm (1940–1960 and 1998–2006) and cool (1905–1925 and 1970–1990) phase periods, separated by transition periods, as identified by Enfield *et al*. (2001). We used regression analysis to determine the amount of variance in the area of 12-month drought explained by monthly values of the PDO and AMO for the 5-year period leading up to the 12-month drought period. We chose the coarser timeframe for drought based on the results of the two-sample *t*-test and based on the idea that the longer periodicity of the PDO and AMO relative to the MEI lends those two indices to an association with more general drought conditions through time.

3. Results

3.1. Trends in drought area

To illustrate the spatial resolution of the HI as dictated by the PRISM data set, we mapped the HI on the occasions of the largest and smallest coverage of abnormally dry conditions and worse ($\leq$40th percentile) in the CRB over the most recent 30 years for the 6-month cool season (November–April) and the 3-month summer monsoon season (July–September) (Figure 4). Using the 6-month HI value for April, dry conditions or worse covered only 0.17% of the CRB in 1993 (Figure 4(a)), but 96.95% in 2002 (Figure 4(b)). Using the 3-month HI for September, dry conditions or worse covered 2.09% of the CRB in 1986 (Figure 4(c)), but 94.61% in 2003 (Figure 4(d)). Graphical and raw data time series of drought area in the CRB are available online at http://www.public.asu.edu/~dellis/hydro_index.html.

Significant positive linear trends in the historical record of monthly drought area in the CRB (not shown) exist for the warm season months of May through August. This agrees with the annual trends for the western United States outlined by Cook *et al*. (2004), and for the southwestern United States as documented by Andreadis and Lettenmaier (2006). The trends are of greater magnitude and statistical significance for the LB than for the UB (Table 3). During the cool season, only the area of the most intense drought in the UB increased significantly on a consistent basis, and this was during the months of January through March.

The increase in warm season drought during the past century is evident when examining seasonal trends in the area of drought based on 3- (HI_3) and 6-month (HI_6) HI values. Significant positive linear trends in area during the summer season (June–August) are evident in the record for the two sub-basins (Table 3). During spring (March–May), the area of the more intense drought conditions increased significantly, particularly for the UB. The area of drought did not increase significantly in either the fall or winter seasons in either of the sub-basins. Using HI_6 values to determine drought area reveals a significant increase in warm season (May–October) drought over the period of record, but no significant trend for the cool season (November–April) (Table 3). When expanding the timeframe to 12-months (HI_{12}), the increase in the area of drought during the warm season is evident, as all trends are significantly positive for all drought categories and for both basins (Table 3).

The increase in the area of warm season drought during the past century was the product of warming rather than drying, which supports the work of Cook *et al*. (2004) who found that the most severe and spatially extensive droughts in the western United States are associated with periods of warmth. Linear trends in air temperature and

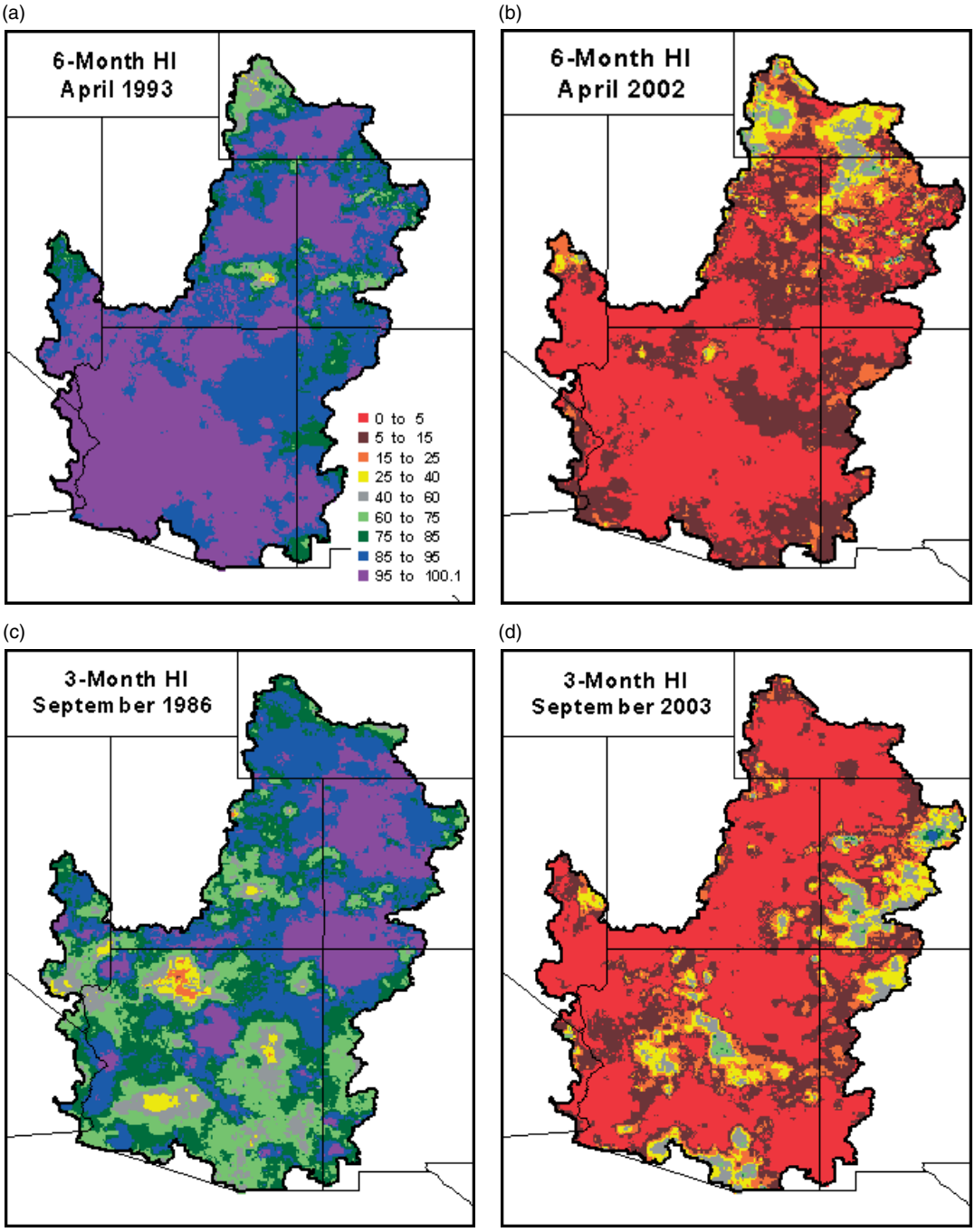

Figure 4. HI values representing 6-month conditions in April 1993 (a) and 2002 (b), and 3-month conditions in September 1986 (c) and 2003 (d). Values on the legend (a) are percentiles.

temperature-driven PE are significantly positive for both basins, regardless of the timeframe considered (Table 4). However, only fall season precipitation in the UB exhibits a significant linear trend, and it is positive, as are nearly all of the seasonal and annual trends. The increased precipitation acted to counter the impact of increasing PE, except during the warm season when PE dominates the regional hydroclimate and drought increased through the period of record.

Much greater percentages of variance in the statistically significant linear trends in the drought coverage are explained by mean basin air temperature than by mean basin precipitation when tested independently. Furthermore, greater variance is explained by temperature in the LB than in the UB. Temperature explains 34.5% (22.4%) of the variance in the linear trend of LB (UB) drought area during the summer season (June–August). In the LB (UB), the explained variance increases to 41.2% (26.0%) for the 6-month warm season (May–October) and 41.6% (26.8%) for the area of 12-month drought. In contrast, on the LB precipitation explains less than 0.1% for the summer season, 0.2% for the 6-month warm season, and 1.0% when using the 12-month timeframe, and values are less on the UB. Time

Table III. Linear trends (percent per decade) in the area of the different levels of drought on the 1-month (all months), 3-month (seasonal), 6-month (warm/cool seasons), and annual timeframes across the upper basin (UB) and lower basin (LB) for the period 1895–2006.

	Dry ≤40th		Moderate ≤25th		Severe ≤15th		Extreme ≤5th	
	UB	LB	UB	LB	UB	LB	UB	LB
1-month (all)	0.6**	1.1**	0.7**	1.4**	0.8**	1.4**	0.5**	0.8**
3-month								
(Dec-)Feb	0.8	1.2	0.7	1.0	0.7	0.6	0.4	0.6
(Mar-)May	1.4	1.5	1.4	1.9	1.0*	1.8	0.5**	1.1*
(Jun-)Aug	2.1*	4.3**	2.1**	3.6**	1.9**	2.7**	1.1**	1.2**
(Sep-)Nov	−0.7	0.1	−0.3	0.6	0.0	0.9	0.1	0.7
6-month								
(Nov-)Apr	0.6	0.7	0.6	1.2	0.7	1.2	0.4	0.7
(May-)Oct	1.6	3.4**	1.7*	3.0**	1.4**	2.4**	0.7**	1.2**
12-month	1.5**	1.2**	1.5**	2.2**	1.3**	2.1**	0.7**	2.1**

Significant trends are noted (* $-p$-value ≤0.05 and ** $-p$-value ≤0.01).

series of the area of 12-month abnormally dry conditions (≤40th percentile) in December along with mean annual air temperature and annual precipitation for the UB and LB are shown in Figure 5. The time series of air temperature (Figures 5(a) and (c)) follow those of drought area better than do the time series of precipitation (Figure 5(b) and (d)).

During the recent 30-year period 1977 through 2006, when warming of the two basins exceeded the century-long rate (Figure 3(a)), we found the following: significant increases in the area of drought in spring rather than summer (Table 5), the increases were of greater significance in the LB than in the UB (Table 5), and precipitation played a greater role in the drought increase than it did for the full period of record. Warming accounted for much of the spring season increase in the area of drought; this result is similar to the role of warming in increasing summer drought area during the 112-year record. Linear trends in air temperature and PE are significantly positive for both basins during the spring season, for the LB summer season, and for both basins during the warm season (May–October) and for each of the longer timeframes (Table 5). In the LB (UB), temperature explains 20.7% (18.9%) of the variance in the linear trend in drought area during the spring season (March–May), increasing to 42.4% (41.3%) for the 6-month warm season (May–October), but decreasing to 36.2% (35.6%) for the 12-month timeframe.

The spring season warming over the period 1977–2006 was accompanied by a significant decrease in precipitation in both basins, but for the longer 12-month timeframe precipitation decreased significantly only in the LB (Table 6). Mean basin precipitation explains 12.8% (9.7%) of the 30-year linear trend in spring drought area in the LB (UB), compared with less than 0.1% for the summer season on the basins over the 112-year period. The percentage increases (decreases) to 15.8% (2.1%) for the 12-month timeframe on the LB (UB), compared with 1.0% or less for the 112-year period.

Table IV. Linear trends in air temperature (°C/decade), potential evapotranspiration (mm/decade), and precipitation (mm/decade) on the 1-month (all months), 3-month (seasonal), 6-month (warm/cool seasons), and annual timeframes across the upper basin (UB) and lower basin (LB) for the period 1895–2006.

	Temperature		Potential Evap		Precipitation	
Timeframe	UB	LB	UB	LB	UB	LB
1-month (all)	0.11**	0.12**	0.36*	0.69**	0.14	0.22
3-month						
(Dec-)Feb	0.14**	0.13**	0.36**	0.60**	−0.30	0.63
(Mar-)May	0.11**	0.13**	0.99**	2.04**	−0.21	0.93
(Jun-)Aug	0.11**	0.13**	2.40**	4.29**	0.42	−0.18
(Sep-)Nov	0.07**	0.09**	0.60**	1.35**	1.83*	1.47
6-month						
(Nov-)Apr	0.11**	0.11**	0.84**	1.44**	0.18	1.44
(May-)Oct	0.10**	0.14**	3.48**	6.84**	1.50	1.44
12-month	0.11**	0.12**	4.32**	8.28**	1.68	2.64

Significant trends are noted (* $-p$-value ≤0.05 and ** $-p$-value ≤0.01).

3.2. ENSO-drought Area

The warm (cool) phase of ENSO, or El Niño (La Niña), is associated with a smaller (larger) area of generally all categories of drought, and the relationship is considerably stronger for the LB than for the UB. There are significant differences in the area of 1-month drought during the two ENSO phases, when considering all months together, but this is due primarily to significant differences during the fall (September–November) season in both basins and also during winter in the LB (Table 7). The significant differences during the fall and winter seasons translate to significant differences in the area of cool season drought during the two ENSO phases, but the contrast is much greater and of greater statistical significance

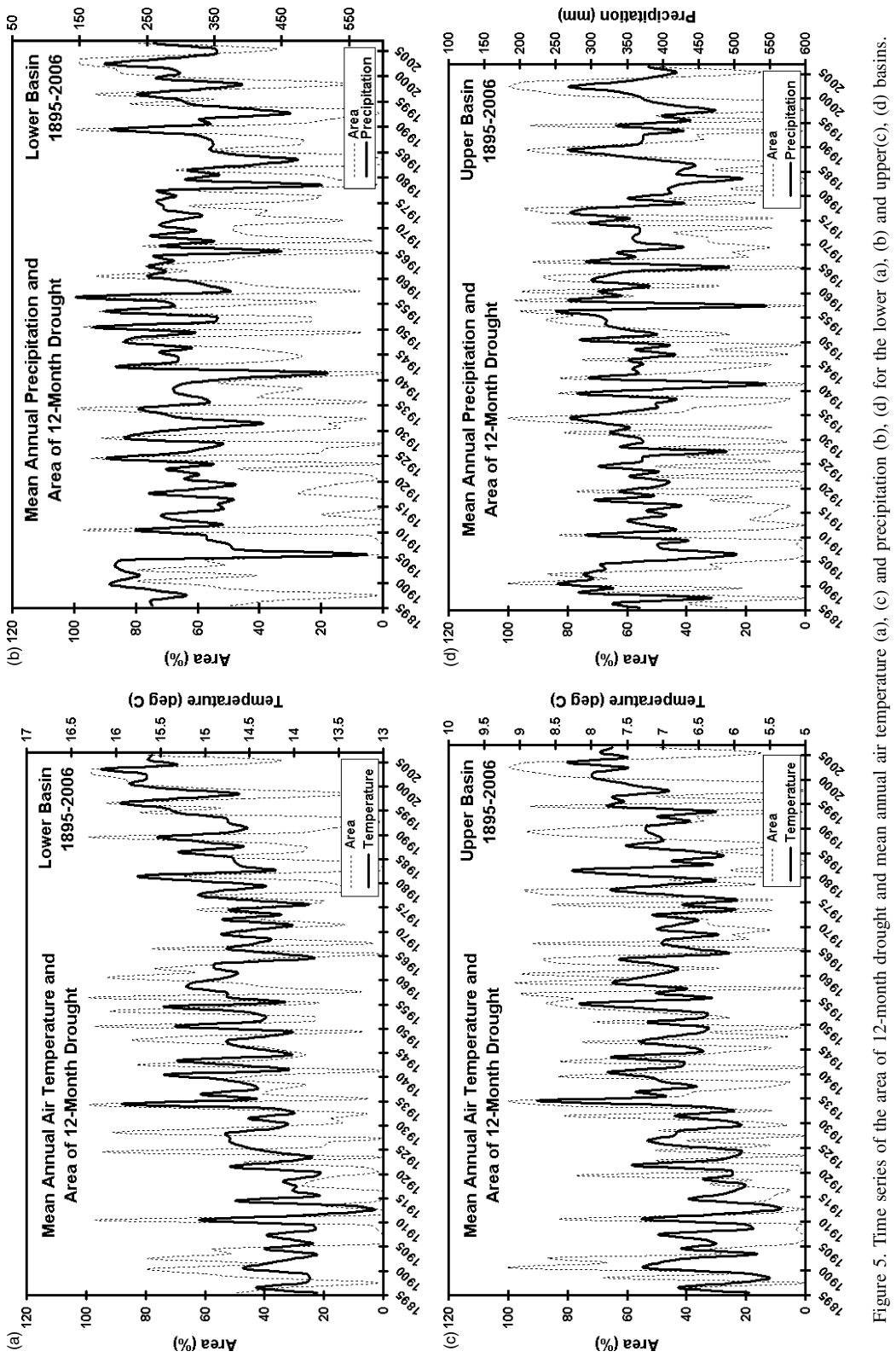

Figure 5. Time series of the area of 12-month drought and mean annual air temperature (a), (c) and precipitation (b), (d) for the lower (a), (b) and upper(c), (d) basins.

Table V. Same as Table III, but for the period 1977–2006.

	Dry ≤40th		Moderate ≤25th		Severe ≤15th		Extreme ≤5th	
	UB	LB	UB	LB	UB	LB	UB	LB
1-month (all)	0.4*	0.9**	0.4*	1.0**	0.4*	0.9**	0.2**	0.5**
3-month								
(Dec-)Feb	0.3	0.7	0.0	0.8	−0.3	1.0	−0.5	0.9
(Mar-)May	1.6*	2.3**	1.2*	1.7**	0.8*	1.2**	0.4*	0.6**
(Jun-)Aug	0.7	1.2	1.0	1.2	1.1	1.2*	0.8	0.8
(Sep-)Nov	−0.4	0.5	−0.1	0.4	0.1	0.4	0.1	0.3
6-month								
(Nov-)Apr	0.5	1.0	0.1	1.0	−0.2	1.1	0.1	0.8
(May-)Oct	0.7	1.5**	0.7	1.7**	0.7	1.8**	0.5	1.2**
12-month	1.0	1.9**	0.9	1.9**	0.8	1.6**	0.5	1.0**

Significant trends are noted (* $-p$-value ≤0.05 and ** $-p$-value ≤0.01).

Table VI. Same as Table IV, but for the period 1977 -2006.

	Temperature		Potential Evap		Precipitation	
Timeframe	UB	LB	UB	LB	UB	LB
1-month (all)	0.32	0.35	1.12	2.29	−0.94	−2.83**
3-month						
(Dec-)Feb	0.36	0.19	0.84	0.78	−2.10	−12.87
(Mar-)May	0.49**	0.59*	5.16**	9.96**	−9.75*	−11.07*
(Jun-)Aug	0.29	0.39*	7.20	13.32**	−1.77	−3.03
(Sep-)Nov	0.13	0.26	0.27	3.57	4.29	−4.56
6-month						
(Nov-)Apr	0.33	0.25	2.58	3.78	−6.42	−23.58
(May-)Oct	0.28*	0.45**	10.74*	23.64**	−0.30	−5.52
12-month	0.32**	0.35**	13.44**	27.48**	−11.28	−33.96*

Significant trends are noted (* $-p$-value ≤0.05 and ** $-p$-value ≤0.01)

in the LB (Table 7). The difference in the area of 12-month drought during the two ENSO phases is not significant in either basin (Table 7), indicating that the ENSO-drought area relationship is confined to seasonal or shorter timeframes.

There is weak short-term predictability of drought area using the MEI. Monthly MEI values preceding the fall season (September–November) explain a statistically significant amount of the variance in the area of fall drought: back to May for the LB, and back to April for the UB (Figure 6(a)). However, there is a large decline in the variance explained when using monthly MEI values prior to June. The variance in fall season drought area explained by monthly MEI values during June through August ranges between only 11 and 13% (Figure 6(a)). MEI values from June through November explain a significant percentage of the variance (based on p-values) in the area of LB winter season (December–February) drought, peaking at greater than 19% in November (Figure 6(b)). The significance of the relationships for both the fall and winter seasons in the LB translates to very significant relationships between cool season (November–April) drought area for the LB and preceding MEI values. Monthly MEI values from May through October explain a significant percentage of the variance in the area of LB cool season drought, peaking at 35% in October (Figure 6(c)). Values are relatively low for the UB, even within the cool season itself.

The strong (weak) relationship between the area of drought and MEI for the LB (UB) is consistent with the literature (Hidalgo and Dracup, 2003; Brown and Comrie, 2004; Balling and Goodrich, 2007; Goodrich, 2007). The positive side of the observed ENSO dipole between the Southwest and Pacific Northwest is centred over the LB while the UB is closer to the axis of the dipole where correlations are not as strong.

3.3. AMO/PDO-drought area

The area of drought within the CRB is larger (smaller) during the warm (cold) phase of the AMO, and the relationship is slightly stronger for the LB than for the UB. The area of 1-month drought is significantly different during the two phases of the AMO, when considering all months together (Table 8). For seasonal timeframes, a significant difference in the area of spring (March–May),

Table VII. Mean area (percent of basin) of the varying degrees of drought during El Niño (EN) and La Niña (LN) phases as indicated by the Multivariate ENSO Index (MEI).

	Dry ≤40th		Moderate ≤25th		Severe ≤15th		Extreme ≤5th	
Upper basin	EN	LN	EN	LN	EN	LN	EN	LN
1-month (all)	34.9	44.7**	22.3	28.5*	13.6	17.5	5.0	6.1
3-month								
(Dec-)Feb	36.9	36.7	21.8	21.3	12.5	11.6	2.9	3.0
(Mar-)May	36.4	49.4	24.3	34.7	15.9	21.0	7.4	6.1
(Jun-)Aug	33.5	46.0	21.0	27.7	14.1	14.3	8.4	3.5
(Sep-)Nov	26.1	49.3*	15.1	35.2*	7.9	23.8*	1.5	9.0*
6-month								
(Nov-)Apr	30.3	54.9*	21.8	33.6	16.4	18.3	9.3	4.1
(May-)Oct	36.3	48.5	24.0	32.9	15.1	20.1	5.7	6.4
12-month	37.3	52.1	26.8	34.0	19.0	20.7	7.9	6.5
Lower basin								
1-month (all)	33.1	47.2**	20.7	31.9**	12.4	21.0**	4.3	7.9**
3-month								
(Dec-)Feb	18.6	58.5**	11.4	38.3**	7.1	22.4*	1.7	10.6
(Mar-)May	33.9	48.2	22.7	30.4	15.6	17.4	7.8	4.6
(Jun-)Aug	41.7	45.0	27.1	27.2	17.5	13.1	8.6	1.5
(Sep-)Nov	31.0	53.1*	16.9	40.2*	10.0	28.0*	3.8	10.8
6-month								
(Nov-)Apr	18.6	64.1**	10.8	45.9**	6.7	30.4**	1.2	10.3*
(May-)Oct	40.1	48.8	27.1	31.5	18.2	18.1	9.0	4.7
12-month	35.0	51.5	23.8	31.9	16.1	18.9	7.5	6.7

Values for each basin are presented for each timeframe, and the significance of the differences is indicated (* $-p$-value ≤0.05 and ** $-p$-value ≤0.01).

summer (June–August), and fall (September–November) LB drought is associated with the two phases of the AMO (Table 8). Only summer exhibits a somewhat consistent statistically significant seasonal drought-AMO relationship on the UB. The difference for the 6-month warm season (May–October) and 12-month timeframe in both basins (Table 8) is statistically greater than for the 1- and 3-month timeframes. This result is consistent with paleoclimate investigations for the western United States (Gray *et al*., 2003; Kitzberger *et al*., 2006), which show synchronous drought and fire, respectively, in association with AMO variations. Investigators suggest that these associations, during summer, may be driven by shifts in atmospheric circulation tied to the thermohaline circulation (Sutton and Hodson, 2005), though other studies suggest that drought in western North America is more closely tied to atmospheric dynamics related to Pacific Ocean forcing (Seager *et al*., 2005).

There is a general tendency for a larger (smaller) area of drought across the CRB during the warm (cold) phase of the PDO, but the relationship is weaker than for either ENSO or AMO. As with both ENSO and AMO, the relationship is strongest for the LB, for which it is consistently significant for the 3-month summer season (July–August) and for the 6-month warm season (May–October) (Table 9). For the UB, only the areas of the more intense drought categories in summer are significantly different during the two phases of the PDO (Table 9). The area of 12-month drought is not significantly different during the two phases of the PDO. The warm phase of the PDO favours a larger drought area during the summer months; however, the relationship is reversed to some extent during the winter (LB) and fall months (UB). While this cool season reversal is not statistically significant for either basin, it appears to be strong enough to offset the warm season drought relationship when examining the 12-month timeframe.

The weakness of the PDO-drought area relationship is in contrast to some literature that relates increased frequency of drought and/or decreased precipitation to the cold phase of the PDO in the CRB (Barlow *et al*., 2001; Hidalgo, 2004; Balling and Goodrich, 2007). Many other investigators found that the PDO only becomes a significant factor in drought frequency for the CRB when the signal reinforces the ENSO or AMO climate signal (Gershunov and Barnett, 1998; McCabe and Dettinger, 1999; Gutzler *et al*., 2002; Hidalgo and Dracup, 2003; McCabe *et al*., 2004; Goodrich, 2007). Newman *et al*. (2003) suggest that PDO is highly ENSO-dependent, and that stratifying the extra-tropical response to ENSO by PDO phase may merely reproduce the ENSO signal plus variations due to weather ('atmospheric white noise' *cf* Newman *et al*., 2003).

The relationship between PDO and drought may be dependent on the method of analysis. An examination of the aforementioned literature shows that the studies

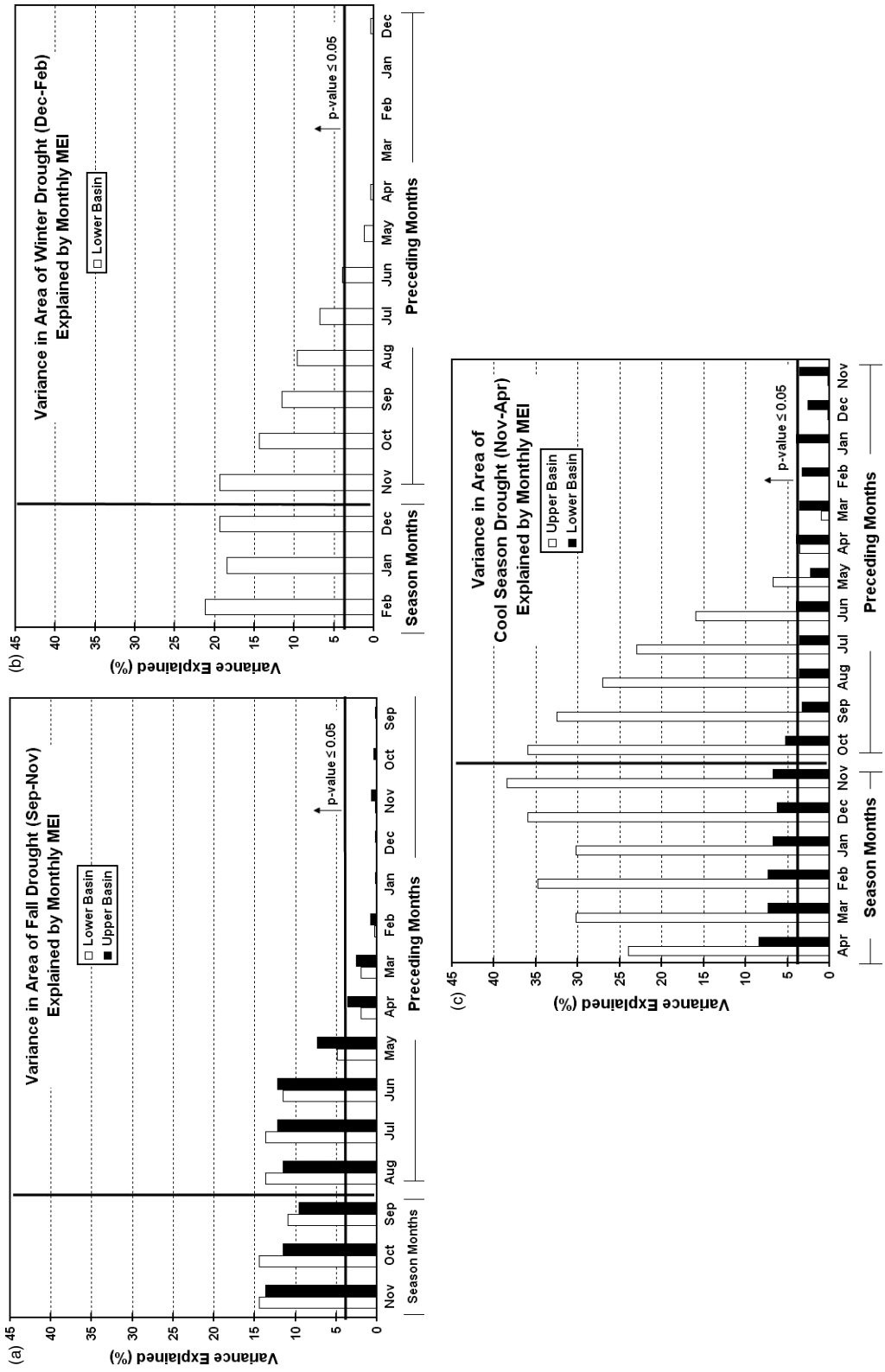

Figure 6. Variance in the area of fall (September–November) (a), winter (December–February) (b), and cool (November–April) (c) season drought explained by monthly values of the Multivariate ENSO Index. Values are given for the months of the season and for the 12 months prior to the beginning of the season. Values for the upper basin are near zero for the winter season and are not shown.

Table VIII. Same at Table VII, but for the warm (positive) and cold (negative) phases of the Atlantic Multi-decadal Oscillation (AMO).

	Dry ≤40th		Moderate ≤25th		Severe ≤15th		Extreme ≤5th	
Upper basin	Warm	Cold	Warm	Cold	Warm	Cold	Warm	Cold
1-month (all)	43.3	36.0**	28.3	21.7**	17.5	12.1**	6.2	3.7**
3-month								
(Dec-)Feb	43.3	36.0	27.2	21.7	15.4	13.3	3.2	4.9
(Mar-)May	47.7	32.4	29.6	20.8	15.9	13.2	3.7	4.7
(Jun-)Aug	48.0	35.9	34.0	19.7*	22.5	9.6*	8.4	2.6
(Sep-)Nov	44.6	32.4	29.7	18.5	18.9	10.0	7.6	2.6
6-month								
(Nov-)Apr	43.5	34.7	28.0	21.6	16.6	13.6	4.6	5.0
(May-)Oct	52.7	30.2**	38.4	17.0**	24.6	8.8**	8.8	2.4*
12-month	51.7	28.7**	35.8	16.5	21.9	9.0*	7.2	2.4
Lower basin								
1-month (all)	46.0	34.2**	32.0	20.0**	21.1	10.8**	8.1	3.2**
3-month								
(Dec-)Feb	44.8	36.3	28.4	20.6	18.0	10.2	7.2	2.4
(Mar-)May	51.4	27.0**	35.3	17.0*	20.3	10.6	10.8	11.2
(Jun-)Aug	49.3	32.9*	34.1	19.4*	22.9	9.6*	8.6	1.7*
(Sep-)Nov	50.3	29.3*	36.5	17.7*	25.2	10.1*	10.1	2.8*
6-month								
(Nov-)Apr	48.7	32.2	33.9	19.3	21.4	10.8	6.7	2.7
(May-)Oct	53.1	28.8**	37.7	17.1**	25.6	8.9**	10.8	1.8*
12-month	53.9	25.6**	38.6	14.6**	25.8	8.0**	10.1	2.1*

Values for each basin are presented for each timeframe, and the significance of the differences is indicated (* $-p$-value ≤0.05 and ** $-p$-value ≤0.01).

Table IX. Same as Table VII, but for the warm (positive) and cold (negative) phases of the Pacific Decadal Oscillation (PDO).

	Dry ≤40th		Moderate ≤25th		Severe ≤15th		Extreme ≤5th	
Upper basin	Warm	Cold	Warm	Cold	Warm	Cold	Warm	Cold
1-month (all)	39.8	39.3	25.6	24.1	15.3	13.8	5.2	4.1
3-month								
(Dec-)Feb	40.0	38.9	24.5	24.5	14.9	14.3	5.4	3.8
(Mar-)May	39.6	39.3	25.0	24.7	15.0	13.9	5.7	3.6
(Jun-)Aug	44.8	34.8	30.7	19.8*	19.7	9.9*	7.1	2.3*
(Sep-)Nov	35.4	43.0	21.6	27.6	12.3	16.3	3.9	5.3
6-month								
(Nov-)Apr	39.8	39.1	25.9	23.3	16.3	13.0	6.2	3.2
(May-)Oct	41.7	37.5	27.8	22.3	17.1	12.1	6.1	3.2
12-month	40.3	38.7	26.4	23.6	16.3	12.8	6.4	2.9
Lower basin								
1-month (all)	40.8	38.4	26.7	23.1*	16.5	12.8**	5.7	3.7**
3-month								
(Dec-)Feb	35.6	42.8	21.2	27.4	12.5	6.4	5.4	4.0
(Mar-)May	41.3	37.9	27.3	22.6	17.4	11.9	7.1	2.4
(Jun-)Aug	48.9	31.3**	33.1	17.7**	21.0	8.7**	7.5	2.0*
(Sep-)Nov	39.9	39.1	25.9	23.9	15.2	13.9	5.0	4.2
6-month								
(Nov-)Apr	37.9	40.9	24.2	24.7	14.9	14.2	6.1	3.3
(May-)Oct	47.3	32.6**	31.6	19.0**	19.5	10.0**	7.2	2.2*
12-month	41.7	37.5	27.6	22.5	17.5	11.7	6.7	2.6

Values for each basin are presented for each timeframe, and the significance of the differences is indicated (* $-p$-value ≤0.05 and ** $-p$-value ≤0.01).

that reflect the strongest relationship between PDO and drought in the CRB focus primarily on the cold-season months (Gutzler *et al*., 2002; Hidalgo and Dracup, 2003; Balling and Goodrich, 2007), whereas weaker relationships are found when seasons are not accounted for (McCabe and Dettinger, 1999; McCabe *et al*., 2004). Our analysis uses monthly, seasonal and annual averages for both the area of drought and PDO and confirms the idea that seasonality contributes to the strength of PDO-drought area relationships. Another possible reason for the lack of a strong cold PDO–CRB drought area relationship in this analysis is that we analysed only the area of drought rather than the severity of drought. Since decades of cold PDO are associated with multi-year La Niñas (e.g. 1954–1956), which often result in multi-year droughts due to negative feedback, any analysis that examined drought severity and PDO would most likely conclude a stronger CRB drought–cold PDO relationship (Cole *et al*., 2002). Additionally, we calculated drought area for regions (LB and UB) that are defined by artificial boundaries determined by a water management compact and not strictly by climate.

Finally, our choice of PDO years likely influenced the outcome as well, as we classified 1977–2006 as a warm PDO phase. There is much uncertainty as to how to categorize the state of the PDO since the strong La Niña of 1998–1999. While it was initially suggested that the PDO had possibly returned to the cold phase in 1998 (Hare and Mantua, 2000), the PDO index became positive in late 2002 and remained in the warm phase through 2006. The inter-annual nature of the PDO since 1998 makes determination of a multi-decadal warm or cold phase problematic, especially considering that the CRB entered into a multi-year drought around this time. If the analysis was re-calculated with the period 1998–2006 as a cold PDO phase, the results show the more typical drought–cold PDO relationship. Owing to this uncertainty, the PDO results should be interpreted with caution.

Given the significance of the relationship between AMO and the area of 12-month drought in both basins, we examined the AMO index as a tool for predicting 12-month drought area. The percentage of variance in the area of drought explained by the monthly AMO index value is higher for the months leading up to the 12-month period than for the concurrent months. This is generally the case for the 4 years prior to the drought period in both the LB and UB, but the percentage of variance explained by the AMO index is highest for the months within 2 years of the drought period in the LB and two and a half years in the UB. Although greater for the LB than the UB, the amount of variance explained is not large in either case, peaking at about 14% at 22 months prior the year in question on the LB, and 13% at 28 months prior on the UB.

The long periodicities of the AMO and PDO make their indices inappropriate for analyses of drought on relatively short timeframes. To better illustrate the relationship of the AMO or PDO with the area of drought on a coarse timeframe, we simply plotted time series of 10-year running means of the variables (Figure 7). Decadal averages of the area of abnormally dry conditions ($\leq$40th percentile) closely follow those of the AMO index for both basins (Figure 7(a) and (b)), but especially for the LB (Figure 7(a)). Ten-year running mean values of the PDO index follow those of drought area for both basins (Figure 7(c) and (d)); however, the first half of the 112-year period exhibits a direct relationship, whereas the last half of the period exhibits an inverse relationship. When compared with the record of the AMO (Figure 7(a) and (b)), this discrepancy may indicate the dominance of the AMO over the PDO in influencing drought in the CRB, as the PDO and AMO have become more in-phase over the last half-century. This may also explain the weaker statistical relationship between the PDO and the area of drought when considering the full historical record. That the AMO may be the more dominant drought influence in the CRB has also been recently supported by McCabe *et al*. (2007). The inverse nature of the PDO–AMO relationship, as the indices relate to drought over the first half of the century, supports previous findings that the drought frequency is higher than average across the southwestern United States when AMO is positive and PDO is negative (Gray *et al*., 2003; Hidalgo, 2004; McCabe *et al*., 2004; McCabe and Palecki, 2006). The latter finding is consistent with modelling studies (e.g. Seager *et al*., 2005), which suggests that ocean temperature variations outside of the tropical Pacific, but forced from the tropical Pacific, act to strengthen North American droughts through interactions between ocean temperatures, poleward Rossby wave propagation, subtropical jets and transient eddies. However, much remains to be learned about the interconnectedness of ENSO, AMO and PDO. While much of the literature (e.g. Seager *et al*., 2005) thus far suggests that the tropical Pacific is the primary driver of North American drought, recent attention has been focused on the importance of the Atlantic basin as a forcing mechanism for drought. Dong *et al*. (2006) describe a mechanism for how the low-frequency changes in the tropical Atlantic may modulate the variability of ENSO via an atmospheric bridge while d'Orgeville and Peltier (2007) propose that multi-decadal variability in the thermohaline circulation in the north Atlantic is responsible for the 60-year cycles found in both the AMO and PDO. Clearly, much work remains to fully understand the physical mechanisms related to low-frequency variability in the extra-tropical oceans, and how they influence drought in the CRB.

4. Summary

The population of the southwestern United States is highly dependent on surface water generated within the arid CRB and therefore sensitive to regional drought. In recent decades the century-long warming of the basin became more rapid, precipitation decreased for a significant portion of the basin, and the regional

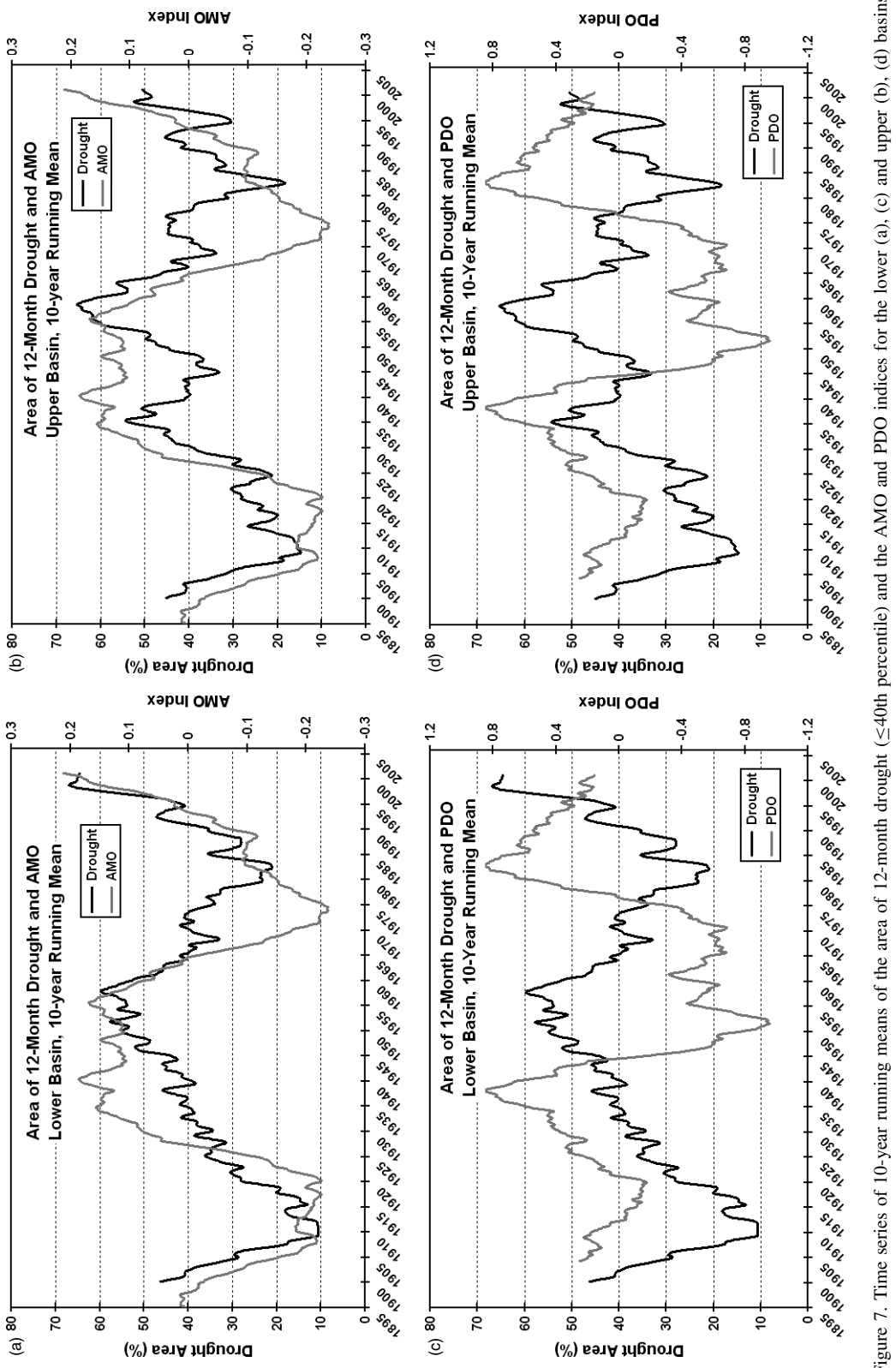

Figure 7. Time series of 10-year running means of the area of 12-month drought (≤40th percentile) and the AMO and PDO indices for the lower (a), (c) and upper (b), (d) basins.

population grew rapidly. Many studies have indicated that runoff in the basin will likely decrease in the future under projected warmer and drier conditions.

To better understand drought occurrence in the CRB we used a hydroclimatic index (HI) to create a historical record of drought area and analysed its linear trend and the relationships between its temporal patterns and key climate teleconnections. The past century was characterized by an increase in the area of drought during the warm portion of the year almost exclusively as a result of climatic warming. In recent decades, the drought coverage increased earlier in the year during spring primarily as a function of warming, but in combination with a decline in precipitation for a significant portion of the basin.

The El Niño (La Niña) phase of the short periodicity ENSO phenomenon is associated with a smaller (larger) area of drought during fall on the upper and lower portions of the basin, during winter in the LB, and during the broader 6-month cool season in both basins. The ENSO phase during the preceding six months is a significant predictor of drought area. The area of drought within the CRB is larger (smaller) during the warm (cold) phase of the longer periodicity AMO. A significant difference in the area of spring, summer, and fall drought in the LB is associated with the two phases of the AMO, while only during summer is a minor relationship evident for the UB. The significance of the difference is greater for the broader 6-month warm season and 12-month timeframe on both basins. There is a general tendency for a larger (smaller) area of drought across the CRB during the warm (cold) phase of the PDO, but the relationship is weaker than for either ENSO or AMO. The relationship is significant for the summer season and the 6-month warm season in the LB. In the UB, only the areas of the more intense drought conditions in summer are significantly different during the two phases of the PDO. The area of the temporally coarser 12-month drought is not significantly different during the two phases of the PDO.

The PDO exhibits little predictive capability, as little variance in drought area is explained by the PDO value for the preceding months. However, the percentage of variance in the area of 12-month drought explained by the monthly AMO index value for the months leading up to the drought period is higher than for the AMO values from the months within the period of drought itself. This is generally the case for the 4 years prior to the drought period, but the percentage of variance explained by the AMO index is highest for the months within 2 years of the drought period on the LB, and two and a half years on the UB. Coarser decadal averages of the area of drought closely follow those of both the AMO and PDO index. However, the nature of the PDO-drought relationship is reversed over the two halves of the historical record, and may indicate a dominance of the AMO over the PDO in influencing drought in the CRB. For each of the three climate teleconnections the relationship with drought area is stronger for the LB than for the UB.

The recent significant increase in drought area across the CRB that coincided with changing phases of the AMO and PDO reinforces the idea of a natural oscillation of regional drought through time. However, the century-long increase in the area of drought and its relationship with increasing regional air temperatures supports the contention of Cook *et al*. (2004) that severe and sustained drought in the western United States is associated with higher air temperature. Andreadis and Lettenmaier (2006) showed that while drought decreased during the 20th century across most of the United States, drought increased across the southwestern portion of the country in response to increased air temperature. The drought-temperature relationship within the CRB, when combined with climate change projections of regional warming could equate to increased fire synchrony across the CRB (Kitzberger *et al*., 2006) and further drought and insect-related forest mortality (Breshears *et al*., 2005). Add a high likelihood of continued population growth to these climate influences and significant long-term water resource problems seem likely for the region.

Acknowledgements

This work was partially funded by the National Oceanic and Atmospheric Administration under grants NA07OAR4310455 and NA07OAR4310460 (Transition of Research Applications to Climate Services), the Bureau of Reclamation under grant 07FG320840, and the National Science Foundation under grant SES-0345945 Decision Center for a Desert City. Any opinions, findings or conclusions expressed in this material are those of the authors and do not necessarily reflect the views of the granting agencies. The authors are grateful for the helpful suggestions of three reviewers.

References

Alley W. 1984. The Palmer Drought Severity Index: limitations and assumptions. *Journal of Climate and Applied Meteorology* **23**: 1100–1109.

Andreadis KM, Clark EA, Wood AW, Hamlet AF, Lettenmaier DP. 2005. Twentieth-century drought in the conterminous United States. *Journal of Hydrometeorology* **6**: 985–1001.

Andreadis KM, Lettenmaier DP. 2006. Trends in 20th century drought over the continental United States. *Geophysical Research Letters* **33**: L10403, DOI:10.1029/2006GL025711.

Balling RC, Goodrich GB. 2007. Analysis of drought determinants for the Colorado River Basin. *Climatic Change* **82**: 179–194.

Barlow M, Nigam S, Berbery EH. 2001. ENSO, Pacific decadal variability, and US summertime precipitation, drought, and stream flow. *Journal of Climate* **14**: 2105–2128.

Breshears DD, Cobb NS, Rich PM, Price KP, Allen CD, Balice RG, Romme WH, Kastens JH, Floyd ML, Belnap J, Anderson JJ, Myers OB, Meyer CW. 2005. Regional vegetation die-off in response to global-change-type drought. *Proceedings of the National Academy of Sciences of the United States of America* **102**: 15144–15148.

Brown DP, Comrie AC. 2004. A winter precipitation 'dipole' in the western United States associated with multidecadal ENSO variability. *Geophysical Research Letters* **31**: L09203, DOI:10.1029/2003GL018726.

Cayan DR, Richmond KT, Riddle LG. 1999. ENSO and hydrologic extremes in the western United States. *Journal of Climate* **12**: 2881–2893.

Christensen NS, Lettenmaier DP. 2006. A multimodel ensemble approach to assessment of climate change impacts on the hydrology and water resources of the Colorado River Basin. *Hydrology and Earth System Sciences Discussion* **3**: 1–44.

Christensen NS, Wood AW, Voisin N, Lettenmaier DP, Palmer RN. 2004. The effects of climate change on the hydrology and water resources of the Colorado River Basin. *Climatic Change* **62**: 337–363.

Cole JE, Overpeck JT, Cook ER. 2002. Multiyear La Niña events and persistent drought in the contiguous United States. *Geophysical Research Letters* **29**(13): 1647, DOI:10.1029/2001GL013561.

Cook ER, Woodhouse CA, Eakin CM, Meko DM, Stahle DW. 2004. Long-term aridity changes in the western United States. *Science* **306**: 1015–1018.

Daly C, Neilson P, Phillips DL. 1994. A statistical–topographical model for mapping climatological precipitation over mountainous terrain. *Journal of Applied Meteorology* **33**: 140–158.

Dickerson WH, Dethier BE. 1970. *Drought Frequency in the Northeastern United States*, Bulletin 596. West Virginia University, Agricultural Experiment Station: Morgantown, WV.

Doesken NJ, Garen D. 1991. *Drought Monitoring in the Western United States Using a Surface Water Supply Index*. Presented at: 7th Conference on Applied Climatology, Sept. 10–13, 1991 in Salt Lake City, Utah and as an Appendix IN Development of a Surface Water Supply Index (SWSI) for the Western United States, 1991. Colorado State University, Dept. of Atmospheric Science: Fort Collins, CO; 77–80.

Dong B, Sutton RT, Scaife AA. 2006. Multidecadal modulation of El Nino-Southern Oscillation (ENSO) variance by Atlantic Ocean sea surface temperatures. *Geophysical Research Letters* **33**: L08705, DOI:10.1029/2006GL025766.

d'Orgeville M, Peltier WR. 2007. On the Pacific Decadal oscillation and the Atlantic multidecadal oscillation: Might they be related? *Geophysical Research Letters* **34**: L23705, DOI:10.1029/2007GL031584.

Easterling DR, Karl TR, Mason EH, Hughes PY, Bowman DP, Daniels RC, Boden TA (eds). 1996. *United States Historical Climatology Network Monthly Temperature and Precipitation Data*. ORNL/CDIAC-87, NDP-019/R3. Carbon Dioxide Information Analysis Center, Oak Ridge National Laboratory: Oak Ridge, TN.

Ellis AW, Hawkins TW, Balling RC, Gober P. 2008. Estimating future runoff levels for a semi-arid fluvial system in central Arizona, USA. *Climate Research* **35**: 227–239.

Enfield DB, Mestas-Nunez AM, Trimble PJ. 2001. The Atlantic multidecadal oscillation and it's relation to rainfall and river flows in the continental U.S. *Geophysical Research Letters* **28**: 2077–2080.

Federer CA, Lash D. 1983. BROOK: a hydrologic simulation model for eastern forests. Research Report No. 19. Water Resources Research Center, University of New Hampshire: Durham, NH.

Federer CA, Vörösmarty C, Fekete B. 1996. Intercomparison of methods for calculating potential evapotranspiration in regional and global water balance models. *Water Resources Research* **32**: 2315–2321.

Garrick G, Jacobs K, Garfin G. 2008. Models, assumptions, and stakeholders: planning for water supply variability in the Colorado River Basin. *Journal of the American Water Resources Association* **44**(2): 381–398.

Gershunov A, Barnett TP. 1998. Interdecadal modulation of ENSO teleconnections. *Bulletin of the American Meteorological Society* **79**: 2715–2725.

Goodrich GB. 2007. Influence of the Pacific decadal oscillation on winter precipitation and drought during years of neutral ENSO in the western United States. *Weather and Forecasting* **22**: 116–124.

Gray S, Betancourt JL, Fastie CL, Jackson ST. 2003. Patterns and sources of multidecadal oscillations in drought-sensitive tree-ring records from the central and southern Rocky Mountains. *Geophysical Research Letters* **30**(6): 1316, DOI:10.1029/2002GL016154.

Guttman NB, Wallis JR, Hosking JRM. 1992. Spatial comparability of the Palmer Drought Severity Index. *Water Resources Bulletin* **28**: 1111–1119.

Gutzler DS, Kann DM, Thornbrugh C. 2002. Modulation of ENSO-based long-lead outlooks of southwestern US winter precipitation by the Pacific Decadal Oscillation. *Weather and Forecasting* **17**: 1163–1172.

Hamon WR. 1961. Estimating potential evapotranspiration. *Proceedings of the American Society of Civil Engineering* **871**: 107–120.

Hare SR, Mantua NJ. 2000. Empirical evidence for North Pacific regime shifts in 1977 and 1989. *Progress in Oceanography* **47**: 103–146.

Heddinghaus TR, Sabol P. 1991. A review of the Palmer Drought Severity Index and where do we go from here?. *Proceedings of the 7th Conference on Applied Climatology*. American Meteorological Society: Boston, MA; 242–246.

Heim RR. 2002. A review of twentieth-century drought indices used in the United States. *Bulletin of the American Meteorological Society* **83**: 1149–1165.

Hidalgo HG. 2004. Climate precursors of multidecadal drought variability in the western United States. *Water Resources Research* **40**: 1–10, DOI:10.1029/2004WR003350.

Hidalgo HG, Dracup JA. 2003. ENSO and PDO effects on hydroclimatic variations of the Upper Colorado River Basin. *Journal of Hydrometeorology* **4**: 5–23.

Hoerling M, Eischeid J. 2006. Past peak water in the southwest. *Southwest Hydrology* **35**: 18–19.

Karl TR. 1986. The sensitivity of the Palmer Drought Severity Index and Palmer's Z-Index to their calibration coefficients including potential evapotranspiration. *Journal of Climate and Applied Meteorology* **25**: 77–86.

Kenney DS, Klein RA, Clark MP. 2004. Use and effectiveness of municipal water restrictions during drought in Colorado. *Journal of the American Water Resources Association* **40**(1): 77–87.

Keyantash J, Dracup JA. 2002. The quantification of drought: an evaluation of drought indices. *Bulletin of the American Meteorological Society* **83**: 1167–1180.

Kitzberger T, Brown PM, Heyerdahl EK, Swetnam TW, Veblen TT. 2006. Contingent Pacific-Atlantic Ocean influence on multicentury wildfire synchrony over western North America. *Proceedings of the National Academy of Sciences* **104**(2): 543–548.

Legates DR, McCabe GJ. 2005. A re-evaluation of the average annual global water balance. *Physical Geography* **26**: 467–479.

Lohani VK, Loganathan GV, Mostaghimi S. 1998. Long-term analysis and short-term forecasting of dry spells by Palmer Drought Severity Index. *Nordic Hydrology* **29**: 21–40.

Lu J, Sun G, McNulty SG, Amatya DM. 2005. A comparison of six potential evapotranspiration methods for regional use in the southeastern United States. *Journal of the American Water Resources Association* **41**: 621–633.

Mantua NJ, Hare SR. 2002. The Pacific decadal oscillation. *Journal of Oceanography* **58**: 35–44.

Mantua NJ, Hare SR, Zhang Y, Wallace JM, Francis RC. 1997. A Pacific interdecadal climate oscillation with impacts on salmon production. *Bulletin of the American Meteorological Society* **78**: 1069–1079.

McCabe GJ, Betancourt JL, Hidalgo HG. 2007. Associations of decadal to multidecadal sea-surface temperature variability with Upper Colorado River flow. *Journal of the American Water Resources Association* **43**: 183–192.

McCabe GJ, Dettinger MD. 1999. Decadal variations in the strength of ENSO teleconnections with precipitation in the western United States. *International Journal of Climatology* **19**: 1399–1410.

McCabe GJ, Palecki MA. 2006. Multidecadal climate variability of global lands and oceans. *International Journal of Climatology* **26**: 849–865.

McCabe GJ, Palecki MA, Betancourt JL. 2004. Pacific and Atlantic Ocean influences on multidecadal drought frequency in the United States. *Proceedings of the National Academy of Science* **101**: 4136–4141.

McCabe GJ, Wolock DM. 2007. Warming may create substantial water supply shortages in the Colorado River basin. *Geophysical Research Letters* **34**: L22708, DOI:10.1029/2007GL031764.

McKee TB, Doesken NJ, Kleist J. 1993. The relationship of drought frequency and duration of time scales. *Eighth Conference on Applied Climatology*. American Meteorological Society: Anaheim, CA; 179–186.

McKee TB, Doesken NJ, Kleist J. 1995. Drought monitoring with multiple time scales. *Ninth Conference on Applied Climatology*. American Meteorological Society: Dallas, TX; 233–236.

Milly PCD, Dunne KA, Vecchia AV. 2005. Global pattern of trends in streamflow and water availability in a changing climate. *Nature* **438**: 347–350.

Nash LL, Gleick P. 1991. The sensitivity of streamflow in the Colorado Basin to climatic changes. *Journal of Hydrology* **125**: 221–241.

Nash LL, Gleick P. 1993. The Colorado River Basin and climate change: The sensitivity of streamflow and water supply to variations in temperature and precipitation. EPA, Policy, Planning, and Evaluation, EPA 230-R-93-009 December.

Newman M, Compo GP, Alexander MA. 2003. ENSO-forced variability of the Pacific Decadal Oscillation. *Journal of Climate* **16**(23): 3853–3857.

Palmer WC. 1965. *Meteorological Drought*. Research Paper No. 45, Weather Bureau, US Department of Commerce, Washington, DC.

Palmer WC. 1968. Keeping track of crop moisture conditions nationwide: the new crop moisture index. *Weatherwise* **21**: 156–161.

Piechota TC, Dracup JA. 1996. Drought and regional hydrologic variation in the United States: Associations with the El Nino Southern Oscillation. *Water Resources Research* **32**: 1359–1373.

Redmond KT, Koch RW. 1991. Surface climate and streamflow variability in the western United States and their relationship to large-scale circulation indexes. *Water Resources Research* **27**: 2381–2399.

Revelle RR, Waggoner PE. 1983. Effects of a carbon dioxide-induced climatic change on water supplies in the western United States. *Changing Climate*. National Academy of Sciences, National Academy Press: Washington, DC.

Ropelewski CF, Halpert MS. 1986. North American precipitation and temperature patterns associated with the El Niño/Southern Oscillation (ENSO). *Monthly Weather Review* **114**: 2352–2362.

Seager R, Kushnir Y, Herweijer C, Naik N, Velez J. 2005. Modeling of tropical forcing of persistent droughts and pluvials over western North America: 1856–2000. *Journal of Climate* **18**: 4065–4088.

Seager R, Ting M, Held I, Kushnir Y, Lu J, Vecchi G. 2007. Model projections of an imminent transition to a more arid climate in southwestern North America. *Science* **316**(5828): 1181–1184.

Shafer BA, Dezman LE. 1982. Development of a surface water supply index (SWSI) to assess the severity of drought conditions in snowpack runoff areas. *Proceedings of the Western Snow Conference* **50**: 164–175.

Steinemann A. 2003. Drought indicators and triggers: a stochastic approach to evaluation. *Journal of the American Water Resources Association* **10**: 1217–1233.

Steinemann AC, Hayes MJ, Cavalcanti LFN. 2005. Drought indicators and triggers. In *Drought and Water Crises: Science, Technology, and Management Issues*, Wilhite DA (ed.). Taylor and Francis: Boca Raton, FL.

Sun G, McNulty SG, Amatya DM, Skaggs RW, Swift LW, Shepard JP, Riekirk H. 2002. A comparison of the hydrology of the coastal forested wetlands and the mountainous uplands in the southern United States. *Journal of Hydrogeology* **263**: 92–104.

Sutton RT, Hodson DLR. 2005. Atlantic Ocean forcing of North American and European summer climate. *Science* **309**(5731): 115–118, DOI: 10.1126/science.1109496.

Thornthwaite CW. 1948. An approach toward a rational classification of climate. *Geographical Review* **38**(1): 55–94.

UNEP. 1992. UNEP, World atlas of desertification. Edward Arnold. London, UK.

USDA Forest Service. 2004. Forest insect and disease conditions in the southwestern region, 2003. Southwestern Region Forestry and Forest Health Pub. No. R3-04-02. http://www.fs.fed.us/r3/publications/documents/fidc2004.pdf (accessed July 13, 2008).

USDOI (U.S. Department of Interior). 2007. Record of decision. Colorado River interim guidelines for Lower Basin shortages and coordinated operations for Lake Powell and Lake Mead. http://www.usbr.gov/lc/region/programs/strategies/RecordofDecision.pdf, accessed July 13, 2008.

Wells N, Goddard S, Hayes MJ. 2004. A self-calibrating palmer drought severity index. *Journal of Climate* **17**(12): 2335–2351.

Wilhite DA, Svoboda MD, Hayes MJ. 2005. Monitoring drought in the United States: status and trends. In *Monitoring and Predicting Agricultural Drought: A Global Study*, Boken VK, Cracknell AP, Heathcote RL Oxford University Press: Oxford, United Kindgom; 121.

Wolock DM, McCabe GJ. 1999. Explaining spatial variability in mean annual runoff in the coterminous United States. *Climate Research* **11**: 149–159.

Wolter K, Timlin MS. 1993. Monitoring ENSO in COADS with a seasonally adjusted principal component index. Proceedings of the 17th Climate Diagnostics Workshop, Norman, OK, NOAA/N MC/CAC, NSSL, Oklahoma Clim Survey, CIMMS and the School of Meteor, Univ of Oklahoma, 52–57.

Xu CY, Singh VP. 2001. Evaluation and generalization of temperature-based methods for calculating evaporation. *Hydrological Processes* **15**: 305–319.

Zhang Y, Wallace JM, Battisti DS. 1997. ENSO-like interdecadal variability: 1900–1993. *Journal of Climate* **10**: 1004–1020.

